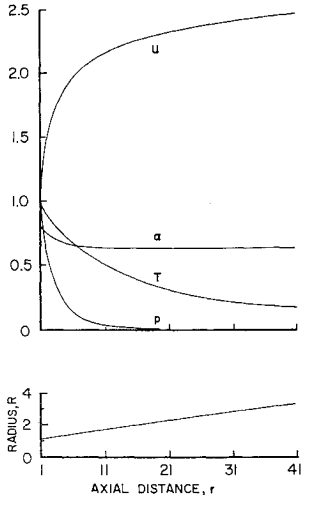

Fig. 1 Nozzle profiles; $(r - 1) = 10\,(1/T - 1)$.

The initial studies of nonequilibrium flow in nozzles was done by Bray,[5] who found that, as the flow temperature dropped, the composition quickly froze as a result of the large decrease in reaction rate. In this problem the same effect is caused by the rapid drop of the Fp/u term as the solution progresses. Since all coupling between the chemical effects and the thermodynamic variables occurs through the reaction equation, the solutions in general do not proceed past the point at which the flow composition freezes. This problem, however, does not exist if the nozzle distance is specified as a function of temperature, as shown on Fig. 1. In this case the nozzle distance is an inverse function of the temperature, and the fact that the rate of change of r was initially large accounts for a relatively gradual change in area near the nozzle throat. An almost conical nozzle with a very short transition at the throat results.

The mass fraction decaying as an inverse temperature function is shown in Fig. 2. Additional results for a variety of cases are given by Widmer.[6] Although these classes of solutions are restricted to that portion of the nozzle prior to the freezing point, the coupling terminates at this point, and there can be no further advantages obtained from geometrical considerations throughout the remainder of the expansion.

The results shown in Figs. 1 and 2 show that the electronic analog computer is a versatile nozzle simulator that conveniently facilitates the variation of specified processes and the rapid exploration through a wide spectrum of flow parameters. Comparison between specified design properties and those actually measured in a prototype nozzle system might afford new insight into the mechanism of real gas flow. In addition, the precise simulation of extreme flight conditions may be obtained more readily in the laboratory by proper nozzle design, although, undoubtedly, viscous effects would have to be considered also.

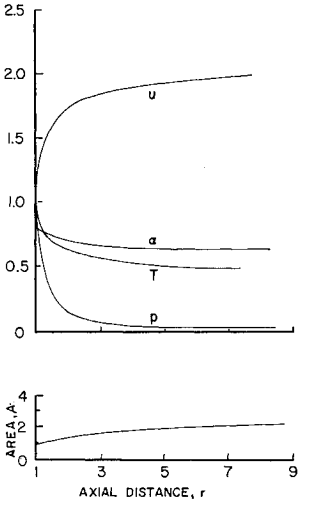

Fig. 2 Nozzle profiles; $(\alpha_0 - \alpha) = 0.15\,(1/T - 1)$.

References

[1] Bray, K. N. C. and Appleton, J. P., "Atomic recombination in nozzles: methods of analysis for flows with complicated chemistry," Univ. Southhampton Rept. AASU 166 (April 1961).

[2] Cambel, A. B., Duclos, D. P., and Anderson, T. P., *Real Gases* (Academic Press Inc., New York, 1963), Chap. 3.

[3] Lighthill, M. J., "Dynamics of a dissociating gas, I: Equilibrium flow," J. Fluid Mech. **2**, 1–32 (1957).

[4] Rink, J. P., Knight, H. T., and Duff, R. E., "Shock tube determination of the dissociation rates of oxygen," J. Chem. Phys. **34**, 1942–1947 (1961).

[5] Bray, K. N. C., "Departure from dissociation equilibrium in a hypersonic nozzle," J. Fluid Mech. **6**, 1–32 (1959).

[6] Widmer, T. E., "The design of hypersonic nozzle contours for reacting flow," M.S. Thesis, Gas Dynamics Lab., Northwestern Univ. (June 1962).

Axisymmetrical Turbulent Jet: Tollmien's Problem Extended

ZEEV ROTEM*
Technion-Israel Institute of Technology, Haifa, Israel

MANY years ago, Tollmien[1, 2] solved the boundary-layer equations for the case of an axisymmetrical jet of incompressible, Newtonian fluid in isothermal, turbulent flow, using Prandtl's mixing-length theory. The case is of considerable interest in the experimental study of turbulence. Recently, a generalized version of Tollmien's equation was solved[3] in a different context, using numerical techniques different from those of Tollmien. Occasion was taken to recompute Tollmien's case, extending considerably the number of points for which numerical results are given, as well as obtaining results for the axial velocity when the kinematic momentum is known and for the axial velocity gradients for which no data had been available. Also, some of the approximations to the accurate boundary-layer solutions made in the earlier work were avoided, and it was thus believed that the present solution would be somewhat more accurate.

The boundary-layer equations for axisymmetrical, incompressible, isothermal flow of a Newtonian fluid are

$$u\frac{\partial u}{\partial x} + v\frac{\partial u}{\partial r} = \frac{1}{\rho}\frac{\partial \tau_{x,r}}{\partial r} \tag{1}$$

$$\frac{\partial u}{\partial x} + \frac{1}{r}\frac{\partial (vr)}{\partial r} = 0 \tag{2}$$

where x is the axial coordinate, r is the radial coordinate, and u and v are the velocity components in the two directions, respectively. The boundary conditions are

$$r = 0 \qquad v = 0 \tag{3a}$$

$$r = 0 \qquad \partial u/\partial r = 0 \tag{3b}$$

$$r = \infty \qquad u = 0 \tag{3c}\dagger$$

Equations (1) and (2) are transformed as follows: assuming Prandtl's mixing-length hypothesis,

$$\frac{\tau_{x,r}}{\rho} = B\left|\frac{\partial u}{\partial r}\right|\frac{\partial u}{\partial r} \tag{4}$$

Received May 9, 1963; revision received August 15, 1963.

* Senior Lecturer, Department of Mechanical Engineering; now at Department of Chemical Engineering, Stanford University, Stanford, Calif.

† Tollmien assumed a *finite* boundary-layer thickness η_R, which, by implication, led to a discontinuity in F''' at $\eta = \eta_R$.

Table 1 Numerical results of integration[a,b]

η	$F'(\eta)/\eta$	$F'(\eta) - F(\eta)/\eta$	$F''(\eta)$	$F''(\eta) - F'(\eta)/\eta$	u/u_0
0.0010	1.36075	0.00068	1.36075	0.00000	1.00000
0.0110	1.36006	0.00748	1.35895	−0.10088	0.99949
0.0210	1.35884	0.01426	1.35592	−0.13928	0.99860
0.0310	1.35730	0.02101	1.35206	−0.16908	0.99746
0.0410	1.35548	0.02774	1.34751	−0.19424	0.99613
0.0510	1.35342	0.05443	1.34239	−0.21638	0.99462

[a] Copies of the complete table may be obtained from the author.
[b] Error: 0.00010; integration checked to 3.4000; infinity at η = 3.4000 [F' (3.4000) = smaller than 10^{-5}]; $F(\infty)$ = 1.54853; $\int_0^\infty [(F')^2/\eta]d\eta$ = 1.000072.

where B is the square of the mixing length, introduce a stream function:

$$u = \frac{1}{r}\frac{\partial\psi}{\partial r} \qquad v = -\frac{1}{r}\frac{\partial\psi}{\partial x} \tag{5}$$

and the similarity transformation:

$$\psi(r,x) = (K/2\pi)^{1/2}(3B)^{1/3}x^{1/3}F(\eta) \tag{6}$$

$$\eta(r,x) = r\cdot(3Bx)^{-1/3} \tag{7}$$

where K is total fluid kinematic momentum:

$$K = 2\int_0^\infty ru^2dr = \text{const} \tag{8}$$

The kinematic momentum must obviously be a constant with x, as constant pressure is assumed. The velocities and the velocity gradients then become

$$u = \left(\frac{K}{2\pi}\right)^{1/2}(3Bx)^{-1/3}\frac{F'(\eta)}{\eta} = \left(\frac{K}{2\pi}\right)^{1/2}\frac{F'(\eta)}{r} \tag{9}$$

$$v = \left(\frac{K}{2\pi}\right)^{1/2}\frac{1}{3x}\left[F'(\eta) - \frac{F(\eta)}{\eta}\right] \tag{10}$$

$$\frac{\partial u}{\partial x} = -\left(\frac{K}{2\pi}\right)^{1/2}\frac{1}{3x}(3Bx)^{-1/3}F''(\eta) \tag{11}$$

$$\frac{\partial u}{\partial r} = \left(\frac{K}{2\pi}\right)^{1/2}(3Bx)^{-2/3}\frac{1}{\eta}\left[F''(\eta) - \frac{F'(\eta)}{\eta}\right] \tag{12}$$

$$\frac{\partial v}{\partial r} = \left(\frac{K}{2\pi}\right)^{1/2}(3Bx)^{-1/3}\frac{1}{3x}\frac{d}{d\eta}\left[F'(\eta) - \frac{F(\eta)}{\eta}\right] \tag{13}$$

$$\frac{\partial v}{\partial x} = -\left(\frac{K}{2\pi}\right)^{1/2}\frac{\eta}{(3x)^2}\frac{d}{d\eta}\left[F'(\eta) - \frac{F(\eta)}{\eta}\right] \tag{14}$$

Equations (1) and (2) now yield the total differential equation:

$$\frac{1}{\eta}\left[FF'' + (F')^2 - \frac{1}{\eta}FF'\right] = \frac{d}{d\eta}\left[\frac{1}{\eta}\left(\frac{F'}{\eta} - F''\right)^2\right] \tag{15}$$

with boundary conditions

$$F' - F/\eta = 0 \qquad \text{at } \eta = 0 \tag{16a}$$

$$(1/\eta)(F'' - F'/\eta) = 0 \qquad \text{at } \eta = 0 \tag{16b}$$

$$F'/\eta = 0 \qquad \text{at } \eta = \infty \tag{16c}$$

It is known that there is no singularity of the functions $F'(\eta)$, $[F''(\eta) - F'(\eta)/\eta]/\eta$, and $[F'(\eta) - F(\eta)/\eta]$ in the flow field. Moreover, obviously, $[F'(\eta)/\eta]_{(\eta=0)} \neq 0$; so the boundary conditions (16) may be simplified to

$$F(0) = 0$$

$$F'(0) = 0 \qquad [F''(0) \pm 0] \tag{17}$$

Table 2 Comparison with Tollmien's data[a]

η	$F'(\eta)/\eta = u/u_0$ Exact	$F'(\eta)/\eta = u/u_0$ Tollmien	$F'(\eta) - F(\eta)/\eta$ Exact	$F'(\eta) - F(\eta)/\eta$ Tollmien
0	1.0000	1.000	0	0
0.0510	0.9946		0.0253	
0.0610	0.9930		0.0302	
0.0625		0.995		0.031
0.0710	0.9912		0.0351	
0.1210	0.9804		0.0588	
0.125		0.977		0.060
0.1310	0.9779		0.0634	
0.250		0.941		0.114
0.2510	0.9421		0.1152	
0.3510	0.9057		0.1520	
0.375		0.895		0.160
0.4010	0.8858		0.1680	
0.5010	0.8435	0.843	0.1949	0.194
0.6010	0.7985		0.2149	
0.625		0.789		0.219
0.6510	0.7753		0.2222	
0.7510	0.7279	0.727	0.2317	0.230
1.0010	0.6072	0.606	0.2261	0.225
1.2510	0.4893	0.487	0.1840	0.182
1.5010	0.3798	0.376	0.1142	0.109
1.7510	0.2822	0.283	0.0271	0.028
2.0010	0.1988	0.198	−0.0669	−0.066
2.2510	0.1305	0.130	−0.1578	−0.159
2.5010	0.0774	0.077	−0.2371	−0.237
2.7510	0.0389	0.039	−0.2979	−0.298
3.0010	0.0142	0.014	−0.3347	−0.334
3.2510	0.0019	0.002	−0.3437	−0.344
3.3510	0.0002		−0.3389	
3.40		0		−0.335

[a] Here $F'(\eta)/\eta|_{\eta=0}$ = 1.00000; $\int_0^\infty [(F')^2/\eta]d\eta$ = 0.540101. Error: 0.00010; integration checked to 3.400; infinity at η = 3.4000 [F'(3.4000) = smaller than 10^{-5}]; $F(\infty)$ = 1.13800. Only part of complete table of calculated data given here.

The remaining constant of integration is obtained from the normalized condition (8):

$$\int_0^\infty \frac{[F'(\eta)]^2}{\eta}d\eta = 1 \tag{18‡}$$

Equation (15) may be integrated immediately once, taking account of (17), to yield

$$FF' = [F'/\eta - F'']^2 \tag{19}$$

Equations (18) and (19) were integrated numerically as a set of three simultaneous nonlinear first-order equations[3] using the Runge-Kutta-Gill method.[4] Results are given (Table 1) and compared to Tollmien's data where possible (Table 2).‡

It is seen that Tollmien's data are surprisingly accurate. The velocity boundary layer thickness, defined to reach to a value of η where the axial velocity had decreased to 1% of its central value, was obtained by interpolation. The numerical value found was 3.063.

Finally, the total flow quantity is obtainable from $F(\infty)$:

$$F(\infty) = (Q/2\pi)(K/2\pi)^{-1/2}\cdot(3Bx)^{-1/3} \tag{20}$$

$F(\infty)$, not given in Ref. 1, was found to be equal to 1.549.

It may be shown[3] that the basic assumptions underlying Eq. (1) will be applicable only for the range

$$[x^2/B]^{-2/3} \ll 1 \tag{21}$$

i.e., $c^{4/3} \ll 1$, where c is the constant of proportionality relating mixing length to the axial coordinate x.

A representative value found experimentally[5] 20 diameters downstream from a turbulent-jet orifice is $c^{4/3} = 4.24 \times 10^{-3}$.

‡ Tollmien uses a different multiplicative constant in his similarity variable η, by normalizing $F'(\eta)/\eta|_{\eta=0}$ instead of (18). Thus data in Table 2 do not satisfy (18).

References

[1] Tollmien, W., "Berechnung turbulenter Ausbreitungsvorgänge," Z. Angew. Math. Mech. 6, 1–12 (1926); also transl. by J. Vanier, "Calculation of turbulent expansion processes," NACA TM 1085, pp. 9–19 (1945).

[2] Pai, S.-I, *Fluid Dynamics of Jets* (D. Van Nostrand Co., Inc., New York, 1954), pp. 105–107.

[3] Rotem, Z., "The axisymmetrical jet of an incompressible pseudoplastic fluid," Appl. Sci. Res. (to be published).

[4] Sepan, A. V., "Runge-Kutta integration," Program Rept. 9, Philco, 24 pp. (1960).

[5] Corrsin, S., "Investigation of flow in an axially symmetrical heated jet of air," NACA W-94, p. 24 (1943).

Minimum Lift-Drag Ratio Required for Global Landing Coverage

RICHARD A. WALLACE* AND WILLIAM A. GRAY†

Boeing Company, Seattle, Wash.

A PRINCIPAL advantage of lifting re-entry vehicles is the lateral range obtained by turning during atmospheric flight. With sufficient lift-drag ratio (L/D), a re-entry glider can land at any desired point on the globe after waiting no longer than one circumnavigation to de-orbit. Higher L/D would not increase landing site selection capability. Therefore, the lowest L/D that provides global coverage might be considered a maximum design goal for lifting re-entry vehicles. As described below, an L/D of 3.6 is found sufficient to land a re-entry glider anywhere on earth, if a particular bank-angle schedule is used.

Determination of this minimum L/D is complicated because the landing footprint is strongly influenced by the choice of enroute bank-angle variation. Thus, the problem becomes one of optimizing the bank-angle schedule for minimum L/D with a terminal constraint for global-landing coverage. Although this problem is amenable to a direct mathematical approach,[1] the procedure chosen was a cut-and-try method guided by past results of such mathematical procedures[2] and past experience with turning trajectories. This procedure gives reasonable results and an insight into the influence of bank-angle schedules on L/D values required for global coverage.

The minimum L/D for global coverage was found for several different bank schedules by plotting the maximum lateral range reached vs L/D and extrapolating to the necessary range for complete global coverage. In Fig. 1 the necessary lateral range is described simply as the ability to reach the North Pole after de-orbiting along the equator. Figure 2 illustrates the four bank-angle schedules that were studied.

In simplified treatments of this problem, a bank-angle of 45° is considered close to optimum. This is satisfactory for L/D less than or equal to 2, but it is unsatisfactory for large L/D and large lateral range.

The bank-angle schedules that depend on heading (Fig. 2a) were found to be the most effective of those tried in accomplishing large lateral range with minimum L/D. Because large bank angles produce quick heading change but also reduce flight range, it seems reasonable to expect that the best bank schedule will incorporate large bank angle to generate initial heading change followed by more moderate bank angle to conserve range.

These trends are confirmed by turn optimization studies[2] for vehicles capable of lateral range on the order of 2000 naut miles (L/D = 2). Gains of around 10% in lateral range are obtained by using an optimum diminishing bank-angle schedule rather than simple 45° bank turns, which appear best in simplified analyses.[3] For global coverage, however, much larger gains are available. Contrast the results in Fig. 1 for 45° bank schedules D or $C2$ with those for diminishing bank-angle schedule $A2$, and note the widening difference in lateral range (as indicated by closer approach to the North Pole) as L/D increases. The superior performance with diminishing bank schedules materially reduces the L/D needed to reach the pole.

Received May 13, 1963.

* Assocate Engineer, Aero-Space Division.

† Now Senior Engineer, North American Aviation Inc., Downey, Calif. Member AIAA.

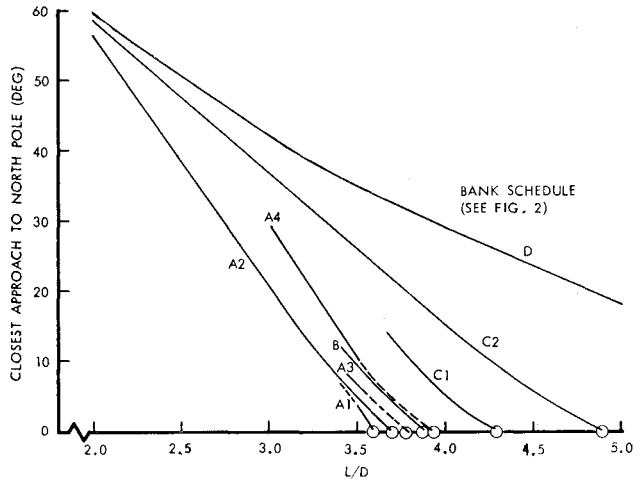

Fig. 1 Necessary lateral range described simply as the ability to reach the North Pole after de-orbiting along the equator.

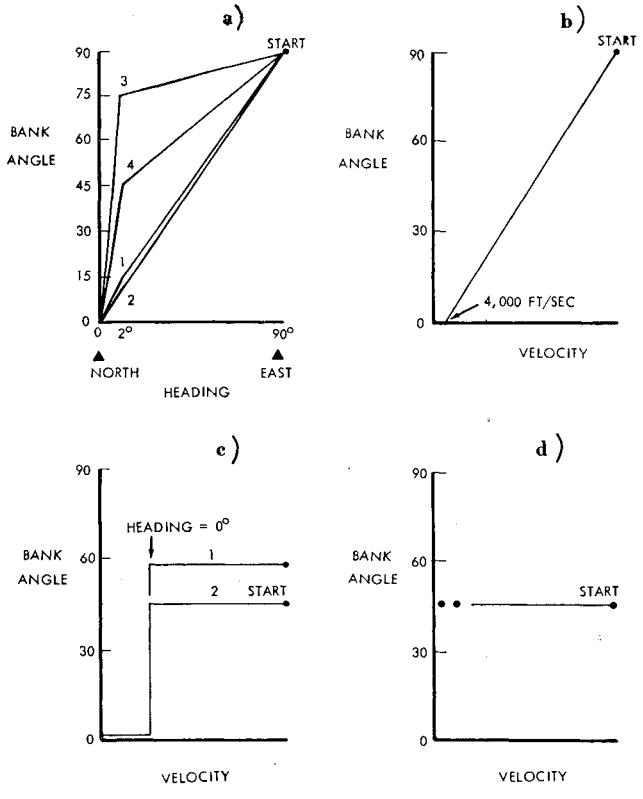

Fig. 2 a) Bank angle varied linearly with heading at two rates: low-rate reduction until the heading equals 2°, then rapid reduction in bank angle as the heading goes to zero (due north). b) Bank angle varied linearly with velocity. c) Bank angle kept constant until heading reaches zero (due north); thereafter the bank angle is kept zero. d) Bank angle kept constant at 45° throughout the flight.